Eur J Plant Pathol (2022) 163:775–787
https://doi.org/10.1007/s10658-022-02514-w

Two distinct leaf anthracnose disease infections in hybrid *Liriodendron* trees in northern China

Guiming Dou · Xing Lü · Fei Ren · Ruhua Li · Dong-Hui Yan

Accepted: 27 April 2022 / Published online: 2 May 2022

Abstract The hybrid tulip tree (*Liriodendron chinense* (Hemsl.) Sarg. × *Liriodendron tulipifera* L.) is one of the most valuable ornamental plants in China. Recently, two leaf anthracnose disease types have emerged on tulip trees in a park in Beijing, China. One type is yellow halo (chlorosis ring) anthracnose characterized by many small round necrotic lesions each of which is circled by a thick chlorosis ring. Lesion spots remain separate from each other even in fallen decaying leaves. Infected leaves turn entirely yellow on trees and then fall immaturely. The other type is non-yellow halo anthracnose characterized by large and irregular necrotic lesions without thick yellow belt margins. Lesions often merge into larger ones during disease development. Infected leaves do not turn yellowish or drop early. The disease pathogens were identified as *Colletotrichum gloeosporioides* sensu stricto strains with multi-loci phylogeny inferences and morphological differences in cultural colonies, conidia, and appressoria. The two types of *Colletotrichum* anthracnose diseases were recorded as novel on *Liriodendron* hosts based on differential characteristics in pathogenic strains, hosts, and disease symptoms. Finally, comprehensive comparisons among all reported leaf diseases on *Liriodendron* trees were performed according to other reported literature.

Keywords Hybrid tulip tree · Anthracnose · *Colletotrichum gloeosporioides* s.s. · Hybrid *Liriodendron* · Northern China

G. Dou · X. Lü · R. Li · D.-H. Yan (✉)
Ecology and Nature Conservation Institute, Key Laboratory of Forest Protection of National Forestry and Grassland Administration, Chinese Academy of Forestry, Beijing 100091, China
e-mail: yandh@caf.ac.cn

F. Ren
Institute of Cereal & Oil Science and Technology, Academy of National Food and Strategic Reserves Administration, Beijing 100037, China

Introduction

Colletotrichum species, with various necrotrophic, hemibiotrophic, and endophytic lifestyles (Jefferies et al., 1990; Kamle & Kumar, 2016; Li et al., 2022; Moreira et al., 2021; Scindiya et al., 2021; Weir et al., 2012), are some of the most important plant pathogens worldwide (Bhunjun et al., 2021; Dean et al., 2012; Jayawardena et al., 2021). The *Colletotrichum gloeosporioides* species complex is especially important due to its ubiquitous occurrence (Choub et al., 2021; Jefferies et al., 1990; Kamle & Kumar, 2016; Khan et al., 2021; Weir et al., 2012). Considering heterogeneity in the species complex, Weir et al. (2012) applied a polyphasic approach that combined morphological characteristics with eight-loci phylogenetic analysis, and segregated the complex into 22 species plus one subspecies, including *C. gloeosporioides* sensu stricto (s.s.) (Jayawardena et al., 2016; Liu et al., 2016; Weir et al., 2012).

Liriodendron tulipifera L. and *Liriodendron chinense* (Hemsl.) Sarg. are ancient relict trees, and the only remaining species of *Liriodendron*. Furthermore, they are important building and ornamental materials because of their excellent texture, unique leaves, and large, beautiful flowers. Hybrid *Liriodendron* is known as an inter-species hybrid between *L. chinense* and *L. tulipifera*, showing greater vigor and better fitness to various environments than its parent lines, and has been planted widely in China (Wang, 1997; Wang et al., 2021). *Liriodendron* spp., including the hybrid species, usually exhibit resistance to biotic or abiotic stresses (Wang, 1997; Wang et al., 2021). However, in recent years, some fungal diseases have been observed. For example, several anthracnoses or brown-spot diseases caused by *Colletotrichum* and other fungi, have been frequently reported on *Liriodendron* foliage in the field (Choi et al., 2012; Kliuchevych et al., 2019; Wang et al., 2013; Zhu et al., 2019). The *Colletotrichum gloeosporiodies* species complex was recorded as pathogens on *L. chinense* in Korea (Choi et al., 2012) and in Ukraine (Kliuchevych et al., 2019), on *L. tulipifera* in Argentina (Lori et al., 2004), and on hybrid *L. chinense* × *tulipifera* in southern China (Zhu et al., 2019). Other *Colletotrichum* pathogens such as *Cerastium acutatum* were reported on *L. tulipifera* in Argentina (Lori et al., 2004), and *Chaetoceros siamense* on *L. chinense* × *tulipifera* in China (Zhu et al., 2019). Apart from *Colletotrichum* spp., *Venturia liriodendra* caused a leafspot disease on *L. tulipifera* in the USA (Hanlin, 1987), and *Physoderma* sp. caused a brown-spot disease on *L. chinense* in China (Wang et al., 2013).

More recently, two anthracnose diseases have been observed on hybrid *Liriodendron* tree foliage growing at Liangshan Park in Beijing, northern China. One disease is symptomatic with round lesion spots circled with yellow halos. Each lesion spot possessed obviously unequal necrotic areas between the upper and lower cuticles, presenting a plain surface on the upper cuticle and a rough surface on the lower cuticle. The rest of the spotted leaves eventually turned yellow and immaturely dropped off. The other disease is characterized by irregular parched necrotic lesions without clear yellow halos, but seldom causes infected leaves to yellow or prematurely drop off. All hybrid *Liriodendron* trees at Liangshan Park showed infection, and the two anthracnose diseases are being found continually throughout Beijing. Besides describing the symptoms, comprehensive comparisons were also performed to distinguish these two anthracnose diseases based on phylogeny, pathogenicity, and biological features of all recorded pathogens and *Liriodendron* spp. hosts.

Materials and methods

Fungal pathogens isolation

Hybrid *Liriodendron* fungal isolates used in this study were randomly collected in August 2020 from diseased leaves of trees growing in Liangshan Park in Beijing, according to the two symptom types observed during the peak disease period. The two symptom types were not observed to co-occur on the same tree. Sampled leaves were rinsed with tap water and surface-sterilized for 1 min in 75% ethanol. Then, symptomatic tissues were cut into segments (3 × 3 mm) along lesion margins. The segments were further surface-disinfested in 3% NaClO for 1 min, 75% ethanol for 30s, rinsed three times in sterile distilled water, air-dried under aseptic conditions, and finally placed on potato dextrose agar (PDA). The cultures were incubated at 25 °C in the dark for 2 to 5 days. Hyphal tips growing from the segments were further transferred to new PDA Petri dishes to form pure colonies. Single-spore cultures were obtained from the pure colonies and examined morphologically (Li et al., 2007). Spores that sporulated from the monosporic colony were used to test pathogenesis.

Pathogenicity assay

Thirty-six *Colletotrichum* isolates were obtained from samples of the two anthracnose diseases. The isolated colonies from the same symptom samples shared almost identical morphological characteristics. Therefore, FPYF3060 and FPYF3062 strains were randomly assigned for pathogenicity assay and morphological description to represent all isolates from the yellowish ring and non-yellow ring symptoms, respectively. The pathogenicity assay was carried out on detached, healthy mature leaves of hybrid *Liriodendron* (Than et al., 2008). Wounds on the leaf surfaces were made with a sterile needle for spore inoculation. Twenty μL of conidial suspension (10^6 spores ml^{-1}) was inoculated onto the wounds. Sterile distilled water was used for control treatments. All inoculated and control leaves were incubated in Petri dishes (150 mm diameter) containing sterilized wet cotton at 25 °C humidity in the dark to observe disease development. Lesions in treated leaves were recorded for seven days after inoculation. The pathogenicity trial was repeated. For matching Koch's postulates, randomly selected lesions tissues were used to re-isolate fungal pathogens for each of the two FPYF3060 and FPYF3062 isolates that were inoculated, according to the procedure described above. The re-isolated FPYF3061 and FPYF3063 fungal isolates were cultured on PDA for microscopically comparing morphological and molecular phylogeny with the original FPYF3060 and FPYF3062 isolates, respectively. The four isolates were further checked for their corresponding identities using morphological characterizations and phylogeny. All treatments and tests were designed with replicate leaves for each isolate and repeated three times.

Morphological analysis

Mycelial discs (5 mm diameter) were taken from the edges of 6-day-old pure culture, placed into petri dishes containing PDA amended with 0.1% yeast extract (PDAY), and incubated at 25 °C in the dark (Han et al., 2016). Growth rate and colony morphology were assessed daily for six, and eighteen days, respectively. Appressoria were generated by conidia suspension on the surface of a hydrophobic slide (Fisher Scientific, Pittsburgh, USA) in vitro. Conidia and appressoria morphological characteristics were observed and measured with a U-TV0.63XC microscope (Olympus, Tokyo, Japan) and Carl Zeiss Microimaging Gmbh 37,081 (Gottingen, Germany).

Molecular identification and phylogenetic analysis

Four isolates (FPYF3060- FPYF3063) were further characterized by DNA sequencing for species verification and identity. Genomic DNA was extracted from each isolate using the CTAB method (Wang et al., 2017). The four-strain genomes were used as templates for PCR amplifying rDNA-ITS (ITS) sequence with ITS-1 (Gardes & Bruns, 1993) and ITS-4 (White et al., 1990) primers, partial glyceraldehyde-3-phosphate dehydrogenase (*GAPDH*) gene with GDF and GDR primers (Templeton et al., 1992), partial calmodulin (*CAL*) gene with CL1C and CL2C primers (Weir et al., 2012), partial actin (*ACT*) gene with ACT-512F and ACT-783R primers (Carbone & Kohn, 1999), partial β-tubulin (*TUB2*) gene with T1 and T2 primers (O'Donnell & Cigelnik, 1997), and partial chitin synthase (*CHS-1*) gene with CHS-79F and CHS-345R primers (Carbone & Kohn, 1999) (Table 1). PCR amplifications were performed with a Bioer LifeEco thermal cycler (BIOER Co., Ltd. Hangzhou, China) in a 25 μl reaction volume. PCR mixtures contained 1 μl DNA template, 0.5 μl of each primer, and 12.5 μl 2× PCR Taq Master Mix (TIANGEN, Beijing, China). PCR reactions for ITS amplification were performed under the following conditions: initial denaturation at 94 °C for 3 min, followed by 35 cycles of 30 s at 94 °C, 45 s at 55 °C plus extension for 1 min at 72 °C, with a final extension step at 72 °C for 5 min. PCR conditions for other loci were the same as for ITS amplification except for the annealing temperatures: *ACT* at 58 °C, *TUB2* at 55 °C, *GAPDH* at 60 °C, *CHS-1* at 58 °C, and *CAL* at 59 °C. PCR products were sequenced with an ABI 3730XL automatic sequencer (Applied Biosystems, USA) by BGI Genomics Co., Ltd. Raw DNA sequences obtained (forward and reverse) were edited and spliced with BioEdit 7.2.5 (Hall, 1999) and then aligned in MAFFT 7 (https://mafft.cbrc.jp/alignment/software/) to form clean sequences for species identification through BLASTn in the NCBI database. All the sequences generated in this study with their accession numbers were deposited in GenBank (Table 2). For phylogenetic inference, all reference sequences from 53 *Colletotrichum* isolates, representing 52 taxa in the *C. gloeosporioides* species complex, from the pathogens recorded on *Liriodendron*, and from the *C. boninense* (ICMP 17904) outgroup were retrieved from GenBank (Choi et al., 2012; Liu et al., 2013; Weir et al., 2012; Zhu et al., 2019) and listed with their NCBI accession numbers in Table 2. A four loci phylogenetic tree generated by neighbor-joining using ITS, *GAPDH*, *ACT*, and *TUB2* sequences in MEGA 7 (Stecher et al., 2016), was constructed based on the Tamura three-parameter model. Relative branch stability was assessed by bootstrapping with 1000 replications. To further discriminate native pathogens from those reported, the phylogeny relationship based on the four genes phylogenetic tree was also tested by ML and MP inferences. The MP tree was constructed using the subtree-pruning-regrafting (SPR) search option with 1000 random sequence additions (level = 1). For the ML tree, the following settings were used: the Tamura 3-parameter model, gamma-distributed (5 categories), and heuristic method using SPR-extensive (Hu et al., 2015). To discriminate our strains from *C. gloeosporioides* s.s. species (Table S1), we also constructed a six-loci phylogenetic tree based on ITS, *GAPDH*, *ACT*, *TUB2*, *CAL,* and *CHS-1*, and a single-locus phylogenetic tree with ITS, or *GAPDH* sequences with the N-J method.

Table 1 Primers used in this study

Gene[z]	Primer	Direction	Sequence (5-3′)	Reference
ACT	ACT-512F	Forward	ATGTGCAAGGCCGGTTTCGC	Carbone & Kohn, 1999
	ACT-783R	Reverse	TACGAGTCCTTCTGGCCCAT	Carbone & Kohn, 1999
CAL	CL1C	Forward	GAATTCAAGGAGGCCTTCTC	Weir et al., 2012
	CL2C	Reverse	CTTCTGCATCATGAGCTGGAC	Weir et al., 2012
CHS-1	CHS-79F	Forward	TGGGGCAAGGATGCTTGGAAGAAG	Carbone & Kohn, 1999
	CHS-345R	Reverse	TGGAAGAACCATCTGTGAGAGTTG	Carbone & Kohn, 1999
GAPDH	GDF	Forward	GCCGTCAACGACCCCTTCATTGA	Templeton et al., 1992
	GDR	Reverse	GGGTGGAGTCGTACTTGAGCATGT	Templeton et al., 1992
ITS	ITS-1	Forward	CTTGGTCATTTAGAGGAAGTAA	Gardes & Bruns, 1993
	ITS-4	Reverse	TCCTCCGCTTATTGATATGC	White et al., 1990
TUB2	T1	Forward	AACATGCGTGAGATTGTAAGT	O'Donnell & Cigelnik, 1997
	T2	Reverse	TAGTGACCCTTGGCCCAGTTG	O'Donnell & Cigelnik, 1997

[z] Actin (*ACT*), calmodulin (*CAL*), chitin synthase (*CHS-1*), glyceraldehyde-3-phosphate dehydrogenase (*GAPDH*), internal transcribed spacer (ITS), and β-tubulin (*TUB2*)

Results

Symptom description

The two anthracnose diseases on hybrid *Liriodendron* had their own unique characteristic symptoms (Fig. 1). During the disease epidemic period, the yellow halo anthracnose type was symptomized by many small necrotic lesion spots with thick yellow halos on leaves (Fig. 1A). Lesion spots were mostly round or near-round and separated from each other. These features remained, even in fallen, initially decaying leaves (Fig. 1A-E). Lesions had unequal necrotic areas on the upper and lower leaf sides, although less obvious on the upper side. The necrotic surface texture on the upper leaf side was touched flat while it was leathery on the lower surface (Fig. 1F-G). Entire diseased leaves eventually turned yellowish and dropped early (Fig. 1B-C). The distinct yellow halos became more obvious on fallen diseased leaves (Fig. 1D-E). The non-yellow halo anthracnose disease type, was marked by fewer, but larger irregular necrotic lesions on infected leaves (Fig. 1H-I). The yellow halo on lesion margins was not observed, nor was fine ring-like chlorosis. This anthracnose disease type did not turn the entire leaf yellowish and they didn't drop early (Fig. 1J). Necrotic cuticles in lesions on fallen leaves became fragile and could easily be cracked in the spot center (Fig. 1K). A single necrotic lesion had an identical area on the upper and lower leaf surfaces. Additionally, there were several concentric rings formed in the lesions (Fig. 1L-M). The two anthracnose diseases were not observed on the same tree.

Fungal isolate pathogenicity

The FPYF3060 strain isolated from the yellow halo type and the FPYF3062 strain isolated from the non-yellow halo type successfully infected host leaf tissues (Fig. 2). Three days after inoculation, tip black spots occurred in leaf wound sites. These spots then gradually developed into overt circular and black necrotic lesions. On day 7, leaf lesions inoculated with strain FPYF3060 were 12.4 mm ($n = 21$, $SD = 0.28$) in average diameter, and produced grainy conidial structures (Fig. 2A). Conversely, leaf lesions inoculated with strain FPYF3062 were 11.7 mm ($n = 21$, $SD = 0.28$) in average diameter, and did not sporulate (Fig. 2B).

FPYF3060 and FPYF3062 morphological characteristics

On PDAY, the FPYF3060 strain formed a circular colony with dense white, fluffy aerial mycelia for 18 days under culture conditions. The reverse side of the colony was white (Fig. 3A). The colony average growth rate was 11.0 mm per day and its conidia were hyaline, straight, cylindrical, obtuse at the apex, truncate at the base, and 14.2 ~ 16.9 × 4.5 ~ 5.8 μm

Table 2 A list of strains used in this study with their sequence's origins

Taxon[z]	Strain	Host	Genebank accession number					
			ITS	*GAPDH*	*CAL*	*ACT*	*CHS-1*	*TUB2*
C. aenigma	**ICMP 18608**	*Persea americana*	JX010244	JX010044	JX009683	JX009443	JX009774	JX010389
C. aenigma	ICMP 18686	*Pyrus pyrifolia*	JX010243	JX009913	JX009684	JX009519	JX009789	JX010390
C. aeschynomenes	ICMP 17673	*Aeschynomene virginica*	JX010176	JX009930	JX009721	JX009483	JX009799	JX010392
C. alatae	ICMP 17919	*Dioscorea alata*	JX010190	JX009990	JX009738	JX009471	JX009837	JX010383
Cryptostemma alienum	ICMP 18691	*P. americana*	JX010217	JX010018	JX009664	JX009580	JX009754	JX010385
C. alienum	ICMP 12071	*Malus domestica*	JX010251	JX010028	JX009654	JX009572	JX009882	JX010411
C. aotearoa	ICMP 17324	*Kunzea ericoides*	JX010198	JX009991	JX009619	JX009538	JX009770	JX010418
C. asianum	ICMP 18696	*Mangifera indica*	JX010192	JX009915	JX009723	JX009576	JX009753	JX010384
C. asianum	ICMP 18580	*Coffea arabica*	FJ972612	JX010053	FJ917506	JX009584	JX009867	JX010406
C. boninense	ICMP 17904	*Crinum asiaticum* var. *sinicum*	JX010292	JX009905	JX009741	JX009583	JX009827	–
C. camelliae	ICMP 10643	*Camellia × williamsii*	JX010224	JX009908	JX009630	JX009540	JX009891	JX010436
Chlerogella clidemiae	ICMP 18706	*Vitis* sp.	JX010274	JX009909	JX009639	JX009476	JX009777	JX010439
C. clidemiae	ICMP 18658	*Clidemia hirta*	JX010265	JX009989	JX009645	JX009537	JX009877	JX010438
C. cordylinicola	ICMP 18579	*Cordyline fruticosa*	JX010226	JX009975	HM470238	HM470235	JX009864	JX010440
Ciboria fructicola	ICMP 17921	*Ficus edulis*	JX010181	JX009923	JX009671	JX009495	JX009839	JX010400
C. fructicola	ICMP 18645	*Theobroma cacao*	JX010172	JX009992	JX009666	JX009543	JX009873	JX010408
C. fructicola	ICMP 18581	*C. arabica*	JX010165	JX010033	FJ917508	FJ907426	JX009866	JX010405
C. fructicola	ICMP 18646	*Tetragastris panamensis*	JX010173	JX010032	JX009674	JX009581	JX009874	JX010409
C. fructicola	ICMP 18613	*Limonium sinuatum*	JX010167	JX009998	JX009675	JX009491	JX009772	JX010388
C. fructicola	ICMP 18120	*D. alata*	JX010182	JX010041	JX009670	JX009436	JX009844	JX010401
C. gloeosporioides	ICMP 17821	*Citrus sinensis*	JX010152	JX010056	JX009731	JX009531	JX009818	JX010445
C. gloeosporioides	ICMP 12939	*Citrus* sp.	JX010149	JX009931	JX009728	JX009462	JX009747	–
C. gloeosporioides	ICMP 12066	*Ficus* sp.	JX010158	JX009955	JX009734	JX009550	JX009888	–
C. gloeosporioides	CG2	***Liriodendron chinense***	JQ238644	–	–	–	–	–
C. gloeosporioides	G2	**Hybrid *Liriodendron***	MK268673	MK268674	–	MK268676	MK268675	–
C. gloeosporioides	CORCG5	***L. chinense***	HM034809	HM034807	HM034803	HM034801	HM034805	HM034811
C. horii	ICMP 12942	*Diospyros kaki*	GQ329687	GQ329685	JX009603	JX009533	JX009748	JX010375
C. horii	ICMP 10492	*D. kaki*	GQ329690	GQ329681	JX009604	JX009438	JX009752	JX010450
C. horii	ICMP 17968	*D. kaki*	JX010212	GQ329682	JX009605	JX009547	JX009811	JX010378
C. kahawae	ICMP 18539	*Olea europaea*	JX010230	JX009966	JX009635	JX009523	JX009800	JX010434
C. kahawae	ICMP 18534	*K. ericoides*	JX010227	JX009904	JX009634	JX009473	JX009765	JX010427
C. kahawae	ICMP 12952	*P. americana*	JX010214	JX009971	JX009648	JX009431	JX009757	JX010426
C. musae	ICMP 17817	*Musa sapientum*	JX010142	JX010015	JX009689	JX009432	JX009815	JX010395
C. musae	ICMP 19119	*Musa* sp.	JX010146	JX010050	JX009742	JX009433	JX009896	HQ596280
C. nupharicola	ICMP 17938	*Nuphar lutea* subsp. polysepala	JX010189	JX009936	JX009661	JX009486	JX009834	JX010397
C. nupharicola	ICMP 18187	*N. lutea* subsp. polysepala	JX010187	JX009972	JX009663	JX009437	JX009835	JX010398

Table 2 (continued)

Taxon[z]	Strain	Host	Genebank accession number					
			ITS	*GAPDH*	*CAL*	*ACT*	*CHS-1*	*TUB2*
C. queenslandicum	ICMP 1778	*Carica papaya*	JX010276	JX009934	JX009691	JX009447	JX009899	JX010414
C. queenslandicum	ICMP 18705	*Coffea* sp.	JX010185	JX010036	JX009694	JX009490	JX009890	JX010412
Colletes salsolae	ICMP 19051	*Salsola tragus*	JX010242	JX009916	JX009696	JX009562	JX009863	JX010403
Chaetoceros siamense	ICMP 17795	*M. domestica*	JX010162	JX010051	JX009703	JX009506	JX009805	JX010393
C. siamense	ICMP 18578	*C. arabica*	JX010171	JX009924	FJ917505	FJ907423	JX009865	JX010404
C. siamense	ICMP 18121	*Dioscorea rotundata*	JX010245	JX009942	JX009715	JX009460	JX009845	JX010402
C. siamense	ICMP 12567	*P. americana*	JX010250	JX009940	JX009697	JX009541	JX009761	JX010387
C. siamense	ICMP 18574	*Pistacia vera*	JX010270	JX010002	JX009707	JX009535	JX009798	JX010391
C. siamense	R3	Hybrids *Liriodendron*	MK268677	MK268678	–	MK268680	MK268679	–
Cataulacus theobromicola	ICMP 17958	*Stylosanthes guianensis*	JX010291	JX009948	JX009598	JX009498	JX009822	JX010381
C. theobromicola	ICMP 18566	*O. europaea*	JX010282	JX009953	JX009593	JX009496	JX009801	JX010376
C. theobromicola	ICMP 18565	*O. europaea*	JX010283	JX010029	JX009594	JX009449	JX009802	JX010374
C. ti	ICMP 5285	*Cordyline australis*	JX010267	JX009910	JX009650	JX009553	JX009897	JX010441
C. ti	ICMP 4832	*Cordyline* sp.	JX010269	JX009952	JX009649	JX009520	JX009898	JX010442
C. tropicale	ICMP 18672	*Litchi chinensis*	JX010275	JX010020	JX009722	JX009480	JX009826	JX010396
C. tropicale	ICMP 18653	*T. cacao*	JX010264	JX010007	JX009719	JX009489	JX009870	JX010407
C. xanthorrhoeae	ICMP 17903	*Xanthorrhoea preissii*	JX010261	JX009927	JX009653	JX009478	JX009823	JX010448
C. gloeosporioides	FPYF3060	**Hybrid *Liriodendron***	MK645985	MK670967	MK674854	MK654907	MK670963	MK670971
C. gloeosporioides	FPYF3061	**Recovered from leaves with FPYF3060 challenged**	MK656105	MK670969	MK674852	MK670961	MK670965	MK670973
C. gloeosporioides	FPYF3062	**Hybrid *Liriodendron***	MK645986	MK670968	MK674855	MK654908	MK670964	MK670972
C. gloeosporioides	FPYF3063	**Recovered from leaves with FPYF3062 challenged**	MK656106	MK670970	MK674853	MK670962	MK670966	MK670974

[z] *C. gloeosporioides* = *Colletotrichum gloeosporioides* = *Glomerella cingulate*. The *Liriodendron* spp. hosts were in bold

(mean 15.6 × 5.1 μm, n = 50) (Fig. 3C). Appressoria were brown, ovoid to irregularly shaped, and 7.4 ~ 8.6 × 6.7 ~ 7.8 μm (mean 8.0 × 7.3 μm, n = 50) (Fig. 3D). On PDAY, the FPYF3062 strain colony was initially white but turned pale gray for 18 days, and the reverse side of the colony was gray in the periphery, deep dark in the middle, and brown/Gy-white in the center. The average growth rate was 12.6 mm per day. The strain initially produced conidial masses around mycelial plugs after incubation for two or three days, and sporulated continuously for 18 days (Fig. 3B). Conidia were cylindrical, straight or slightly curved with round ends, single-celled, and 12.1 ~ 13.6 × 4.3 ~ 4.9 μm (on average 12.9 × 4.6 μm, n = 50) (Fig. 3E). Appressoria were oval-shaped, 7.2 ~ 8.9 × 5.9 ~ 6.7 μm (on average 8.0 × 6.3 μm, n = 50), and brown (Fig. 3F). The morphological characteristics of the re-isolated

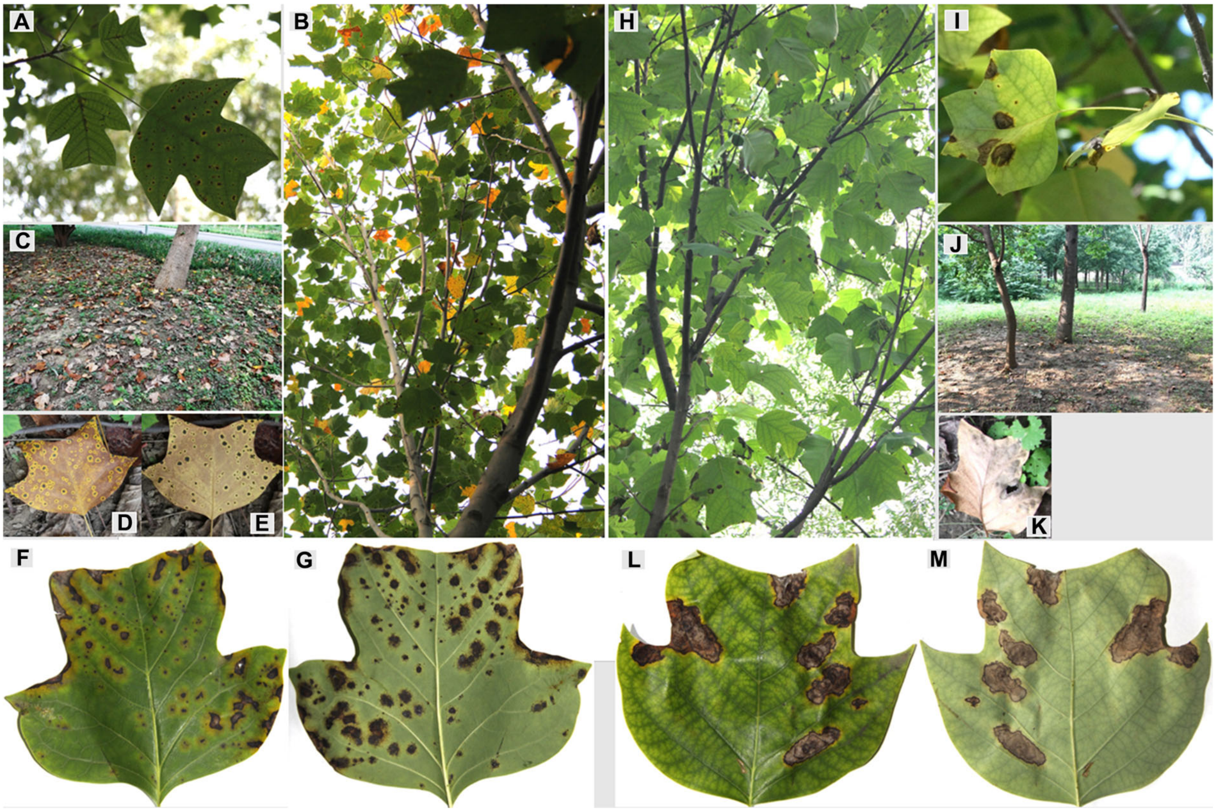

Fig. 1 The symptoms of two types of anthracnose diseases on leaves of hybrid Liriodendron. **A** and **B**, disease symptom of etiolation (yellow halo) anthracnose on trees in the field. **C**, heavy defoliation caused by etiolation anthracnose. **D** and **E**, the upper and lower sides of fallen diseased leaves of etiolation anthracnose. **F** and **G**, the obverse and reverse sides of an etiolation anthracnose leaf. **H** and **I**, disease symptoms of non-etiolation (non-yellow halo) anthracnose on trees in the field. **J**, much less defoliation caused by non-etiolation anthracnose. **K**, the hole on fallen diseased leaf of non-etiolation anthracnose. **L** and **M**, the obverse side and reverse side of non-etiolation anthracnose leaf

FPYF3061 strain were identical to the original FPYF3060 strain used for pathogenicity assay. The FPYF3063 strain was also identical to the original FPYF3062 strain challenge agent for the pathogenicity test (data not shown).

Molecular identification and phylogenetic analysis

Four-loci phylogenetic inference, based on *GAPDH*, *ACT*, *TUB2,* and ITS region genes, showed that native FPYF3060–3063 isolates were clustered with

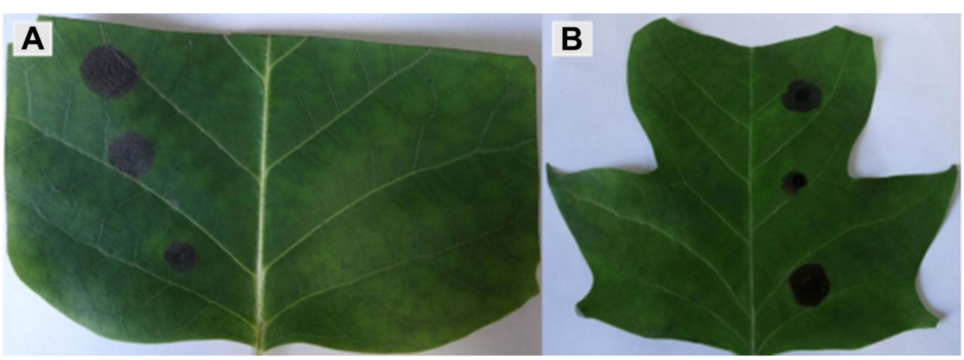

Fig. 2 Symptoms observed in pathogenicity tests after artificial inoculation on detached leaves caused by **A,** FPYF3060. **B,** FPYF3062

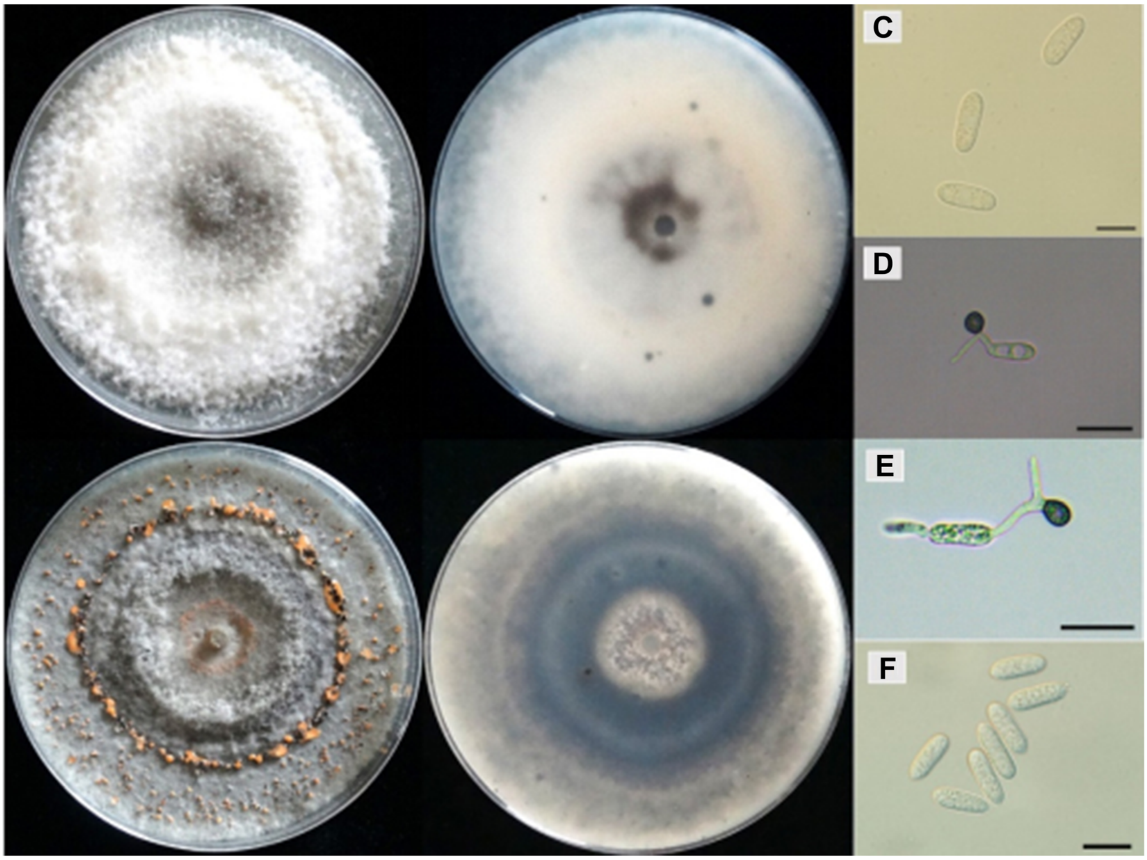

Fig. 3 The morphological characteristics of isolates FPYF3060 and FPYF3062 on PDAY in dark for 18 days. **A,** View of the upper and reverse sides of FPYF3060 colony on PDAY. **B,** View of the upper and reverse sides of FPYF3062 colony on PDAY. **C and D,** The conidia (scale bar = 10 μm) and appressoria (scale bar = 20 μm) of FPYF3060. **E and F,** The conidia (scale bar = 10 μm) and appressoria (scale bar = 20 μm) of FPYF3062

C. gloeosporioides s.s. in a clade by 98% support, however, they could also be ascribed into different subclades within the clade (Fig. 4). The FPYF3062 and FPYF3063 isolates were grouped into a subclade with 96% bootstrap value. The FPYF3060 and FPYF3061 isolates were grouped into another subclade with 85% bootstrap value, and at a certain distance to the terminal cluster grouped with *C. gloeosporioides* s.s. type strains. Therefore, the phylogenetic relationships of the native pathogens with yellow and non-yellow halo symptoms suggest that they have phylogenetic linkages within the *C. gloeosporioides* s.s. clade, but differential phylogenetic linages.

Discussion

Molecular identifications using ITS sequencing analysis, protein-encoding genes, and phylogenetic inferences determined that native fungal isolates FPYF3060–3063 on anthracnose diseased leaves of hybrid *Liriodendron* were strains from *C. gloeosporioides* s.s. (Fig. 4, Fig. S1-S4). Their colony, conidia, and appressoria morphological features were also consistent with descriptions of the *C. gloeosporioides* s.s. epitype (Cannon et al., 2008). Their pathogenicity on hybrid *Liriodendron* was verified via Koch's postulates, with the same strains being successfully re-isolated (Figs. 2 and 3). In the pathogenicity test, symptoms associated with yellow halo disease did not fit well with strain FPYF3060, partly because detached leaf physiology could be inadequate to explain the yellowish occurrence, such as from insufficient light (Liu et al., 2007; Zhu et al., 2019). Furthermore, although the two native strains were determined as *C. gloeosporioides* s.s. species, their colony characteristics showed many differences in texture, color, and productivities (Fig. 3A-B, Table S2), which were distinct in phylogeny subclades

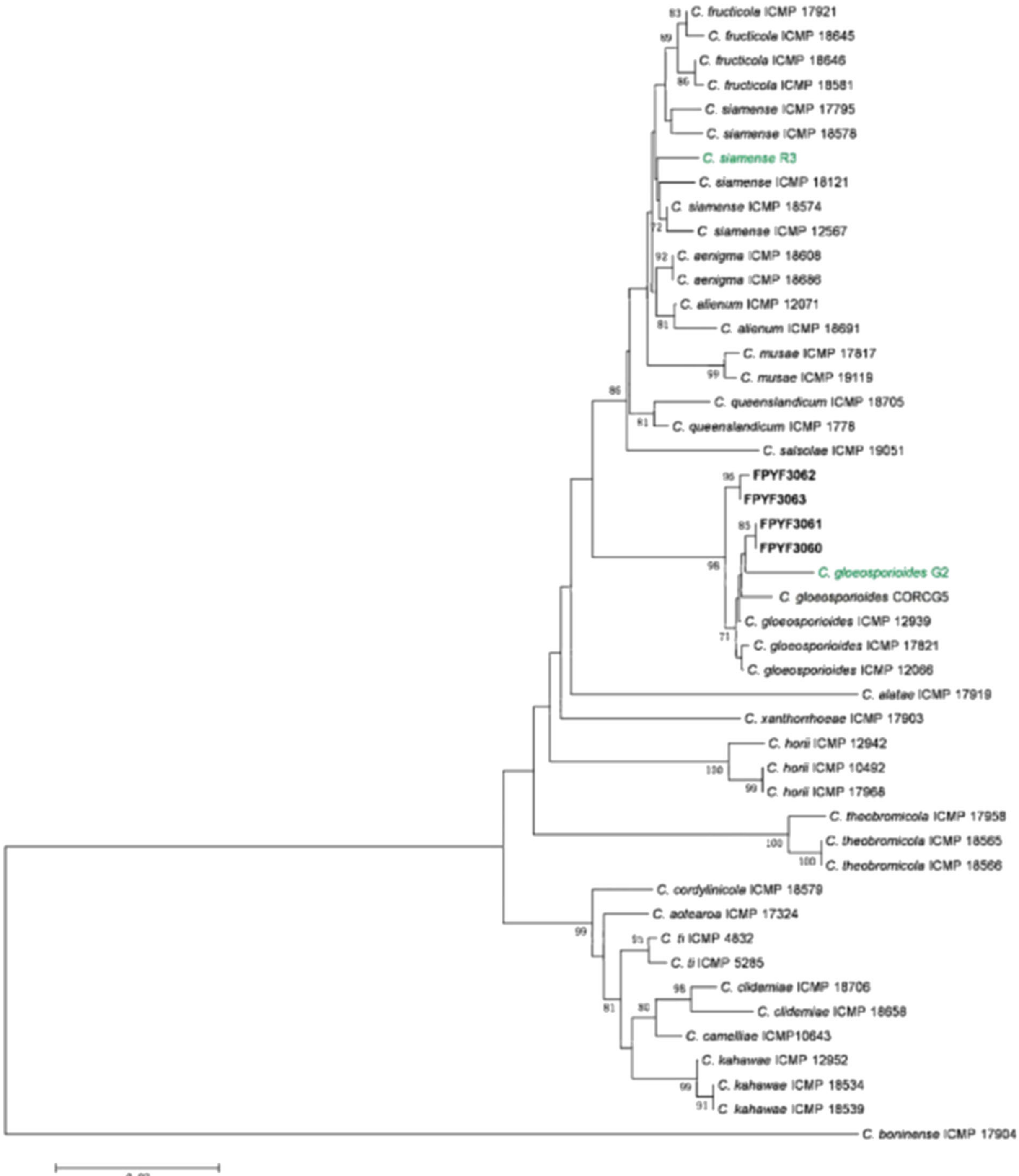

Fig. 4 Phylogenetic tree based on neighbor-joining using MEGA7. The tree was built using concatenated data from four sequences of ITS, *GAPDH*, *ACT*, and *TUB2* of the strains FPYF3060- FPYF3063. *C. boninense* is used as outgroup. Bootstrap values >70% (1000 replications) marked at the nodes. Bar = 0.02 substitutions per nucleotide position. Our four strains are in bold. Those pathogenic strains reported by Zhu et al. (2019) were marked in green

(Fig. 4, Fig. S1-S4). The strain FPYF3062 (FPYF3063) phylogeny even suggested that *C. gloeosporioides* s.s. could be divided into distinctive genetic groups (Bhunjun et al., 2021; Weir et al., 2012) (Fig. 4). The six-loci phylogenetic tree (Fig. S1) and other phylogenetic relationships (Fig. S2-S4) together showed the same result. Therefore, the *Colletotrichum* pathogens from the yellow and non-yellow halo anthracnose diseases were different (Fig. 4, Fig. S1, Table S2).

On *Liriodendron* hosts, several leaf spot diseases have been documented including those caused by *Colletotrichum* spp.. Hanlin (1987) recorded that *Venturia liriodendra* caused leafspot disease on *L. tulipifera* (Hanlin, 1987). More recently, Zhu et al. (2019) reported *C. gloeosporioides* strain G2 and *C. siamense* strain R3 infections on hybrid *Liriodendron* growing in southern China. Kliuchevych et al. (2019) detected *C. gloesporioides* s.s. on *L. chinense* in Ukraine. Fu et al. (2020) tested the pathogenicity of *C. gloeosporioides* strain Lc1 isolated from *L. chinense* host tree leaves, and demonstrated that it was able to cause leaf spots. However, some significant differences exist in the diseases presented in this paper compared to those pathogens or/and symptoms already documented (Tables S2-S3, Fig. S5). For symptoms, only the disease on tulip trees in Ukraine seemed to be highly similar to our yellow halo anthracnose diseases (Fig. S5), but its hosts were *L. chinense*, not hybrid *L. chinense* × *tulipifera* trees. Moreover, the Ukraine *Colletotrichum* pathogen formed sporulations on the leaves (Kliuchevych et al., 2019) while our *Colletotrichum* pathogens were not observed to sporulate on necrotic lesions throughout the diseased period even on fallen infected leaves in the field (Fig. 1). However, there was no information on phylogenetic molecular marker sequences (even ITS) available for the Ukraine *C. gloesporioides* strain (Kliuchevych et al., 2019). There are clearly different symptoms (Table S3, Fig. S5) and pathogens (Table S2) for anthracnose diseases on hybrid *Liriodendron* trees between southern and northern China (Fu et al., 2020; Zhu et al., 2019). Phylogenetic relationships based on the single locus, such as ITS or *GPADH*, and multi-loci concatenated sequences of four or six marker molecular sequences make it clear that native FPYF strains from northern China are distinct from pathogens of *C. gloeosporioides* s.s. strains from southern China (Fig. S1-S4, Fig. 4). Notably, except for phylogeny trees based on single ITS sequences showing uncertain relationships for all *C. gloeosporioides* s. s. strains (Fig. S6), all multi-loci phylogenetic trees robustly supported that the strains FPYF3060–3063, on the hybrid *Liriodendron* hosts from northern China have evolved a unique distance phylogeny within the *C. gloeosporioides* s. s. clade (Fig. S2-S4). Strain FPYF3062 (FPYF2063), the pathogenic agent of non-yellow halo anthracnose, diverged early from almost all reported *C. gloeosporioides* s. s. strains. Moreover, there were differences in conidia and appressoria size between our two strains (FPYF3060 (FPYF3061) and FPYF3062 (FPYF3063)) and the southern strain *C. gloeosporioides* G2 (Table S2) (Zhu et al., 2019). These complementary comparisons further confirm that the strain FPYF3060 (FPYF3061) or FPYF3062 (FPYF3063) on hybrid *Liriodendron* hosts in northern China is not identical to those reported on hosts in southern China (Zhu et al., 2019). As for other pathogens documented on *Liriodendron* hosts, *Colletotrichum gloeosporioides* CG2 in Korea cannot be a *C. gloeosporioides* species, but could be *C. aotearoa* according to its phylogenetic characterization (Fig. S7). The CG2 strain had smaller conidia and appressoria than strains FPYF3060 and FPYF3062 (Table S2) (Choi et al., 2012). The pathogen *Colletotrichum acutatum* LPS47188 on *L. tulipifera* from Argentina also had smaller conidia than our strains (Lori et al., 2004, Table S2), but no data was available for appressoria comparison. The pathogenic strain, *Colletotrichum gloeosporioides* Lc1, which was isolated from *L. chinense* hosts and recently genome sequenced (Fu et al., 2020), exhibited a distinctive distance from our strains in phylogenetic relationships (Fig. S2). Finally, the two *Colletotrichum* anthracnose disease types in this paper were easily discriminated by their different symptoms (Fig. 1). According to our observations, in the field the two types were seldom observed co-occurring on the same tree, although they randomly infected hosts within hybrid *Liriodendron* populations at the same time. We expect to explore the specificity between the pathogens and hosts in the future.

Conclusions

In view of their polyphyletic nature (Bhat et al., 2018; Bhunjun et al., 2021; Jayawardena et al., 2016; Weir et al., 2012), *Colletotrichum gloeosporioides* strains on hybrid *Liriodendron* hosts growing in northern China exhibited an obvious phylogenetic distance with those documented on three tulip tree host species based on detailed molecular phylogenetic analyses (Fig. 4, Fig.

S1-S4), conidial features (Fig. 3, Table S2) and unique symptoms (Fig. 3, Fig. S5) (Choi et al., 2012; Fu et al., 2020; Hanlin, 1987; Kliuchevych et al., 2019; Lori et al., 2004; Wang et al., 2013; Zhu et al., 2019). The yellow and non-yellow halo anthracnose diseases on hybrid *Liriodendron* in northern China also had two distinctive types of foliage spots (Fig. 3, Fig. S5). Although anthracnose disease had been reported on hybrid *Liriodendron* hosts in Nanjing, a city in south-eastern China (Zhu et al., 2019), the anthracnose pathogens in northern hybrid *Liriodendron* hosts were distanced from the southern strains in pathogenic genetics (Fig. S2-S6). Moreover, the non-yellow halo anthracnose caused by the *C. gloeosporioides* s.s. strain FYPF3062 (3063) on hybrid *Liriodendron* in Beijing in northern China, was symptomatically distinct from reported anthracnose diseases on the same host species in southern regions (Fig. S5) (Choi et al., 2012; Fu et al., 2020; Kliuchevych et al., 2019; Wang et al., 2013; Zhu et al., 2019). Therefore, the two *Colletotrichum gloeosporioides* diseases on hybrid *Liriodendron* hosts in northern China were confirmed to be novel types of anthracnose leaf spots. Both diseases could significantly degrade hybrid *Liriodendron* landscapes in northern China. Recent, frequent reports of *Colletotrichum* spp. pathogenic diseases emerging on *Liriodendron* tulip trees are alarming in the present world of global climate change. Urgent, preventative measures are required for *Colletotrichum* spp. disease management.

Supplementary Information The online version contains supplementary material available at https://doi.org/10.1007/s10658-022-02514-w.

Acknowledgments This research was funded by DEVELOPMENT PROJECT OF ECOLOGY AND NATURE CONSERVATION INSTITUTE, CAF, grant number 99813-2020 and YOUTH FUND PROJECT OF NATIONAL SCIENCE FOUNDATION OF CHINA, grant number 31901316. Mr. Zheng Wang and Mrs. Shimeng Tan are acknowledged for their support and help in constructing phylogenetic trees. We also appreciate Miss. Danran Bian for her help in pathogenic test.

Availability of data and material All data generated or analysed during this study are included in this published article [and its supplementary information files].

Code availability Not applicable.

Funding DEVELOPMENT PROJECT OF RESEARCH INSTITUTE OF FOREST ECOLOGYY, ENVIRNMENT AND PROTECTION, CAF, grant number 99813–2020 and YOUTH FUND PROJECT OF NATIONAL SCIENCE FOUNDATION OF CHINA, grant number 31901316.

Declarations

Conflicts of interest/competing interests The authors declare no conflict of interest.

Research involving human participants and/or animals Not applicable.

Informed consent Not applicable.

References

Bhat, N. N., Mahiya, F., Padder, B. A., Shah, M. D., Dar, M. S., Nabi, A., Bano, A., Rasool, R. S., & Sana, S. (2018). Microsatellite mining in the genus *Colletotrichum*. *Gene Reports, 13*, 84–93. https://doi.org/10.1016/j.genrep.2018.09.001

Bhunjun, C. S., Phukhamsakda, C., Jayawardena, R. S., Jeewon, R., Promputtha, I., & Hyde, K. D. (2021). Investigating species boundaries in *Colletotrichum*. *Fungal Diversity, 107*, 107–127. https://doi.org/10.1007/s13225-021-00471-z

Cannon, P. F., Buddie, A. G., & Bridge, P. D. (2008). The typification of *Colletotrichum gloeosporioides*. *Mycotaxon, 104*, 189–204.

Carbone, I., & Kohn, L. M. (1999). A method for designing primer sets for speciation studies in filamentous ascomycetes. *Mycologia, 91*, 553–556. https://doi.org/10.2307/3761358

Choi, O., Choi, O., Kwak, Y. S., Kim, J., & Kwon, J. H. (2012). Spot anthracnose disease caused by *Colletotrichum gloeosporioides* on tulip tree in Korea. *Mycobiology, 40*, 82–84. https://doi.org/10.5941/MYCO.2012.40.1.082

Choub, V., Maung, C. E. H., Won, S. J., Moon, J. H., Kim, K. Y., Han, Y. S., Cho, J. Y., & Ahn, Y. S. (2021). Antifungal activity of cyclic tetrapeptide from *bacillus velezensis* CE 100 against plant pathogen *Colletotrichum gloeosporioides*. *Pathogens, 10*(2), 209. https://doi.org/10.3390/pathogens10020209

Dean, R., Van-Kan, J. A. L., Pretorius, Z. A., Hammond-Kosack, K. E., Di-Pietro, A., Spanu, P. D., Rudd, J. J., Dickman, M., Kahmann, R., Ellis, J., & Foster, G. D. (2012). The top 10 fungal pathogens in molecular plant pathology. *Molecular Plant Pathology, 13*, 414–430. https://doi.org/10.1111/j.1364-3703.2012.00822.x

Fu, F. F., Hao, Z., Wang, P., Lu, Y., Xue, L., Wei, G., Tian, Y., Hu, B., Xu, H., Shi, J., Cheng, T., Wang, G., Yi, Y., & Chen, J. (2020). Genome sequence and comparative analysis of *Colletotrichum gloeosporioides* isolated from *Liriodendron* leaves. *Phytopathology, 110*, 1260–1269. https://doi.org/10.1094/PHYTO-12-19-0452-R

Gardes, M., & Bruns, T. D. (1993). ITS primers with enhanced specificity for basidiomycetes-application to the identification of mycorrhizae and rusts. *Molecular Ecology, 2*, 113–118. https://doi.org/10.1111/j.1365-294X.1993.tb00005.x

Hall, T. A. (1999). BioEdit: A user-friendly biological sequence alignment editor and analysis program for windows 95/98/ NT. *Nucleic Acids Symposium Series, 41*, 95–98. https://doi.org/10.1021/bk-1999-0734.ch008

Han, Y. C., Zeng, X. G., Xiang, F. Y., Ren, L., Chen, F. Y., & Gu, Y. C. (2016). Distribution and characteristics of *Colletotrichum* spp. associated with anthracnose of strawberry in Hubei, China. *Plant Disease, 100*, 996–1006. https://doi.org/10.1094/PDIS-09-15-1016-RE

Hanlin, R. T. (1987). *Venturia liriodendri* sp. nov., associated with a leafspot disease of *Liriodendron*. *Mycologia, 79*, 464–467. https://doi.org/10.2307/3807473

Hu, M. J., Grabke, A., & Schnabel, G. (2015). Investigation of the *Colletotrichum gloeosporioides* species complex causing peach anthracnose in South Carolina. *Plant Disease, 99*, 797–805. https://doi.org/10.1094/PDIS-10-14-1076-RE

Jayawardena, R. S., Hyde, K. D., Damm, U., Cai, L., Liu, M., Li, X. H., Zhang, W., Zhao, W. S., & Yan, J. Y. (2016). Notes on currently accepted species of *Colletotrichum*. *Mycosphere, 7*, 1192–1260. https://doi.org/10.5943/mycosphere/si/2c/9

Jayawardena, R. S., Hyde, K. D., de Farias, A. R. G., Bhunjun, C. S., Ferdinandez, H. S., Manamgoda, D. S., Udayanga, D., Herath, I. S., Thambugala, K. M., Manawasinghe, I. S., Gajanayake, A. J., Samarakoon, B. C., Bundhun, D., Gomdola, D., Huanraluek, N., Sun, Y., Tang, X., Promputtha, I., & Thines, M. (2021). What is a species in fungal plant pathogens? *Fungal Diversity, 109*(1), 239–266. https://doi.org/10.1007/s13225-021-00484-8

Jefferies, P., Dodd, J. C., Jeger, M. J., & Plumbley, R. A. (1990). The biology and control of *Colletotrichum* species on tropical fruit crops. *Plant Pathology, 39*, 343–366. https://doi.org/10.1111/j.1365-3059.1990.tb02512.x

Kamle, M., & Kumar, P. (2016). *Colletotrichum gloeosporioides*: Pathogen of anthracnose disease in mango (*Mangifera indica* L.). In P. Kumar, V. Gupta, A. Tiwari, & M. Kamle (Eds.), *Current trends in plant disease diagnostics and management practices* (pp. 207–219). Springer-Cham. https://doi.org/10.1007/978-3-319-27312-9_9

Khan, M. R., Chonhenchob, V., Huang, C., & Suwanamornlert, P. (2021). Antifungal activity of propyl disulfide from neem (*Azadirachta indica*) in vapor and agar diffusion assays against anthracnose pathogens (*Colletotrichum gloeosporioides* and *Colletotrichum acutatum*) in mango fruit. *Microorganisms, 9*(4), 839. https://doi.org/10.3390/microorganism9040839

Kliuchevych, M. M., Chumak, P. Y., Vigera, S. M., & Stolyar, S. G. (2019). First detection of *Colletotrichum gloesporioides* (Penz.) pens. & Sacc. On *Liriodendron chinense* (Hemsl.) Sarg. In Ukraine. *Modern Phytomorphology, 13*, 9–12.

Li, M. F., He, J., Ding, L., Kang, J. C., Zhang, Q., & Zheng, Q. W. (2007). Single spore strains without producing fruit body isolated from *Cordyceps militeris* and their RAPD analysis. *Southwest China Journal of Agricultural Sciences, 20*, 547–550.

Li, N., Xu, D., Huang, R., Zheng, J., Liu, Y., Hu, B., Gu, Y., & Du, Q. (2022). A new source of Diterpene lactones from *Andrographis paniculata* (Burm. F.) Nees-two endophytic Fungi of *Colletotrichum* sp. with antibacterial and antioxidant activities. *Frontiers in Microbiology, 13*. https://doi.org/10.3389/fmicb.2022.819770

Liu, F., Damm, U., Cai, L., & Crous, P. W. (2013). Species of the *Colletotrichum gloeosporioides* complex associated with anthracnose diseases of *Proteaceae*. *Fungal Diversity, 61*, 89–105. https://doi.org/10.1007/s13225-013-0249-2

Liu, F., Wang, M., Damm, U., Crous, P. W., & Cai, L. (2016). Species boundaries in plant pathogenic fungi: A *Colletotrichum* case study. *BMC Evolutionary Biology, 16*, 81. https://doi.org/10.1186/s12862-016-0649-5

Liu, G., Kennedy, R., Greenshields, D. L., Peng, G., Forseille, L., Selvaraj, G., & Wei, Y. (2007). Detached and attached *Arabidopsis* leaf assays reveal distinctive defense responses against hemibiotrophic *Colletotrichum* spp. *Molecular Plant-Microbe Interactions, 20*, 1308–1319. https://doi.org/10.1094/MPMI-20-10-1308

Lori, G. A., Alippi, A. M., & Dimenna, S. (2004). First report of species of *Colletotrichum* causing leaf blotch of *Liriodendron tulipifera* in Argentina. *Plant Disease, 88*, 1381. https://doi.org/10.1094/PDIS.2004.88.12.1381A

Moreira, R. R., Zielinski, E. C., Castellar, C., Bergamin Filho, A., & May De Mio, L. L. (2021). Study of infection process of five species of *Colletotrichum* comparing symptoms of glomerella leaf spot and bitter rot in two apple cultivars. *European Journal of Plant Pathology, 159*(1), 37–53. https://doi.org/10.1007/s10658-020-02138-y

O'Donnell, K., & Cigelnik, E. (1997). Two divergent intragenomic rDNA ITS2 types within a monophyletic lineage of the fungus *fusarium* are nonorthologous. *Molecular Phylogenetics and Evolution, 7*, 103–116. https://doi.org/10.1006/mpev.1996.0376

Scindiya, M., Malathi, P., Kaverinathan, K., Sundar, A. R., & Viswanathan, R. (2021). Knock-down of glucose transporter and sucrose non-fermenting gene in the hemibiotrophic fungus *Colletotrichum falcatum* causing sugarcane red rot. *Molecular Biology Reports, 48*(3), 2053–2061. https://doi.org/10.1007/s11033-021-06140-3

Stecher, G., Kumar, S., & Tamura, K. (2016). MEGA7: Molecular evolutionary genetics analysis version 7.0 for bigger datasets. *Molecular Biology and Evolution, 33*, 1870–1874. https://doi.org/10.1093/molbev/msw054

Templeton, M. D., Pikkerink, E. H. A., Solon, S. L., & Crowhurst, R. N. (1992). Cloning and molecular characterization of the glyceraldehyde-3-phosphate dehydrogenase encoding gene and cDNA from the plant pathogenic fungus *Glomerella cingulata*. *Gene, 122*, 225–230. https://doi.org/10.1016/0378-1119(92)90055-T

Than, P. P., Jeewon, R., Hyde, K. D., Pongsupasamit, S., Mongkolporn, O., & Taylor, P. W. J. (2008). Characterization and pathogenicity of *Colletotrichum* species associated with anthracnose on chilli (*Capsicum* spp.) in Thailand. *Plant Pathology, 57*, 562–572. https://doi.org/10.1111/j.1365-3059.2007.01782.x

Wang, J. X., Ma, L. J., Zhang, L. Q., & Mao, S. F. (2013). Pathogen identification of the brown-spot disease of *Liriodendron chinensis*. *Scientia Silvae Sinica, 49*, 189–191. https://doi.org/10.11707/j.1001-7488.20130628

Wang, K. Y., Strobel, G. A., & Yan, D. H. (2017). The production of 1,8-cineole, a potential biofuel, from an endophytic strain of *Annulohypoxylon* sp. FPYF3050 when grown on agricultural residues. *Journal of Sustainable Bioenergy Systems, 7*, 65–84. https://doi.org/10.4236/jsbs.2017.72006

Wang, P., Dong, Y., Zhu, L., Hao, Z., Hu, L., Hu, X., Wang, G., Cheng, T., Shi, J., & Chen, J. (2021). The role of γ-aminobutyric acid in aluminum stress tolerance in a woody plant, *Liriodendron chinense× tulipifera*. *Horticulture Research, 8*, 80. https://doi.org/10.1038/s41438-021-00517-y

Wang, Z. R. (1997). Genetic resources preservation and breeding prospect of *Liriodendron chinense*. *Forest Science and Technology, 9*, 8–10.

Weir, B. S., Johnston, P. R., & Damm, U. (2012). The *Colletotrichum gloeosporioides* species complex. *Studies in Mycology, 73*, 115–180. https://doi.org/10.3114/sim0011

White, T. J., Bruns, T., Lee, S., & Taylor, J. W. (1990). Amplification and direct sequencing of fungal ribosomal RNA genes for phylogenetics. In M. A. Innis, D. H. Gelfand, J. J. Sninsky, & T. J. White (Eds.), *PCR protocols: A guide to methods and applications* (pp. 315–322). Academic Press.

Zhu, L. H., Wan, Y., Zhu, Y. N., Huang, L., & Liu, C. L. (2019). First report of species of *Colletotrichum* causing leaf spot of *Liriodendron chinense × tulipifera* in China. *Plant Disease, 103*, 1431. https://doi.org/10.1094/PDIS-12-18-2265-PDN